Journal of Applied Polymer Science

Effects of poly(dimethyl siloxane) on the water absorption and natural degradation of poly(lactic acid)/oil-palm empty-fruit-bunch fiber biocomposites

John Olabode Akindoyo, Mohammad Dalour Hossen Beg, Suriati Ghazali, Muhammad Remanul Islam
Faculty of Chemical and Natural Resources Engineering, Universiti Malaysia Pahang, Lebuhraya Tun Razak, Gambang 26300, Kuantan, Malaysia
Correspondence to: M. Beg (E-mail: dhbeg@yahoo.com)

ABSTRACT: Composites were fabricated with poly(lactic acid) and oil-palm empty-fruit-bunch (EFB) fibers with extrusion; this was followed by an injection-molding technique. Before compounding, the surface of the fiber was modified through ultrasound and poly(dimethyl siloxane) (PDMS). The influences of the ultrasound and PDMS on the water absorption and biodegradability of the composites were investigated. Additionally, the composites were buried under soil for 6 months, and their biodegradability was assessed through different characterization techniques, such as tensile testing and weight loss and diffussability measurement. The changes on the surface of the fibers due to treatment were examined by scanning electron microscopy analysis, and the influences on the biodegradability of the composites were observed. Functional group analysis and possible changes before and after degradation were also examined by a Fourier transform infrared spectrophotometric technique. The results analyses revealed that the treatment of fibers improved the density of the fibers and reduced the water uptake of the composites. The overall weight loss due to soil burial testing was found to be maximum for the untreated-fiber-based composites (6.8%), whereas the ultrasound- and silane-treated composites showed the minimum value of weight loss (3.7%). The deterioration of the tensile strength due to degradation was found to be at a maximum for the untreated-fiber-based composite (27%), whereas the ultrasound- and silane-treated-fiber-based composites showed a minimum value of 8%. © 2015 Wiley Periodicals, Inc. J. Appl. Polym. Sci. **2015**, *132*, 42784.

KEYWORDS: biodegradable; composites; extrusion; fibers; properties and characterization

Received 15 April 2015; accepted 28 July 2015
DOI: 10.1002/app.42784

INTRODUCTION

Over the years, a lot of disturbance and damage has been experienced by the ecosystem as a result of advancing technology, which has promoted the use of more nondegradable materials. This threat to the environment has become huge, to the extent that much legislation on sustainability to favor the environment is being enacted by the day. Manufacturing industries, especially the packaging, construction, and automobile industries, are, therefore, involved in a compulsory search for new environmentally friendly biodegradable alternatives that can effectively replace their conventional synthetic nonbiodegradable counterparts. Thus, the production of cheap and environmentally compliant engineering materials is being sought as the most feasible and convenient alternative.[1] This could be possible through the incorporation of natural fiber as reinforcements in polymer composites for the fabrication of degradable plastic composites.[2] On the basis of these advantages of natural fibers, which also include low cost, biodegradability, low density, and desirable mechanical properties, several composites materials have been fabricated. Natural fibers, such as jute, sisal, hemp, pineapple, coir, abaca, date palm, kenaf, and oil-palm empty-fruit-bunch (EFB) fibers, have been used for composite fabrication.[3]

EFB fiber is a hard and tough fiber, which is in many ways similar to coir fiber,[4] and the surface of EFB fibers has many pores; these offer it great interlocking properties with the polymer matrix during composite fabrication. However, the presence of its porous surface morphology could lead to high water absorption by capillary action whenever it is exposed to water.[5] Moreover, the hydrophilic tendencies of EFB fibers could lead to poor interfacial bonding between the fibers and the matrix during composite fabrication.[6] It is, therefore, necessary to apply appropriate surface modification through physical or chemical processes to enhance the adhesion between the hydrophilic fibers and the hydrophobic matrix.[3] One chemical treatment method that has proven to have a high effectiveness for fiber surface modification is treatment with ultrasound and silane

coupling agents.[7,8] In a different study, alkali treatment was carried out followed by silane modification of EFB-fiber-based poly(lactic acid) (PLA) composites.[9] Result analysis revealed improved interfacial adhesion as result of enhanced mechanical properties of the formulated biocomposite. Similar results were obtained by other researcher for PLA-based biocomposites.[10] Except for the interfacial adhesion between the fibers and matrix, the brittleness of the PLA-based composites were found to be reduced through an increase in toughness due to the incorporation of different fibers as fillers for PLA-based composites.[11]

On the other hand, PLA is a thermoplastic polymer that is degradable. It possesses desirable mechanical properties, and it has begun to be produced on a large scale through the fermentation of lactic acid from corn followed by chemical polymerization. The degradability of PLA comes from its ability to be broken down into carbon dioxide, water, and some other smaller molecules in the environment[1] within a period of several months to around 2 years. Other petroleum-based plastics, however, need 500–1000 years to fully degrade in the environment. Although the biodegradation of PLA and its composites is often said to be a complex phenomenon with a relatively slow rate, PLA can, however, be biodegraded into water and carbon dioxide under composting conditions.[12,13] The degradation process can be enhanced by the stimulation of an acidic or basic environment and in the presence or with contact with high moisture and high temperature.[14,15] The hydrolytic degradation of PLA-based rice hull composites were analyzed, and the result show that degradation depended mostly on a higher water temperature.[16] The molecular weight of PLA decreased from 153.1 kDa to 10.7 kDa with hydrolysis of the ester group.

Biodegradation studies of polymer composites have revealed that moisture absorption is a common phenomenon with all composites a humid atmosphere or whenever they are immersed in water. This often leads to degradation at the interfacial regions of the fiber and matrix and creates reduced stress-transfer efficiency and a possible subsequent reduction in both mechanical and dimensional properties.[2] Generally, the diffusion of moisture in polymer composites is governed by three mechanism vis-à-vis the flow of water molecules into the microcracks between the polymer chain and the transport of water through capillarity action into cracks and gaps at the fiber–matrix interfacial region.[17] This is often due to poor mechanical bonding during composite fabrication and, last, the transport of microcracks within the composite, arising from fiber swelling within the composite. These factors could instigate undesired degradation of composite materials if they are not properly managed.

The objective of this study was to investigate the role of fiber treatment in the degradation behavior of PLA and its composites with EFB fibers through water uptake and soil burial analysis. EFB fibers, which were surface-modified through concurrent ultrasound and poly(dimethyl siloxane) (PDMS) treatment, were incorporated into a PLA matrix for degradation analysis. The effects of fiber treatment on the biodegradation of the composites and the consequences of biodegradation on the mechanical properties of the composite were also investigated.

EXPERIMENTAL

Materials

EFB fibers were collected from LKPP Corp. Sdn. Berhad Kuantan (Malaysia). PLA (3051D biopolymer grades of Nature Works Ingeo) was purchased from Unic Technology, Ltd. (China). The supplied PLA had a melt flow index density of 30–40 g/10 min (190°C/2.16 kg), a melting temperature of 160–170°C, a density of 1.24 g/cm^3, and a molecular weight of 204,453 g/mol. Sodium hydroxide (analytical grade), acetic acid, and acetone were procured from Merck (Germany), whereas PDMS was purchased from Sigma Aldrich. PDMS is a colorless liquid with a viscosity of 3.0 cSt, a relative density of 1.0 g/cm^3 (at room temperature), a flash point of 85°C, and a boiling point of 177°C/760 mmHg.

Methods

Fiber Treatment and Composite Fabrication. The treatment of EFB fiber was carried out through modification with ultrasound followed by silane treatment. For ultrasound treatment, the fibers were weighed and put into a beaker containing a solution of 2 wt % NaOH to maintain a fiber-to-water ratio of 1 : 20. The beaker and its content were placed inside an ultrasound bath (CREST Ultrasonics), and treatment was conducted at 90°C for 100 min at an ultrasound power of 9 W/cm^2. The treated fibers were thoroughly washed in a water flow to remove excess alkali. As washing was continued, a few drops of a very dilute acetic acid solution were added until the waste wash water no longer revealed signs of alkalinity, that is, until pH 7 was reached. Furthermore, ultrasound-treated empty-fruit-bunch fibers (UTFs) were treated with PDMS. For this treatment, the fibers were soaked in a solution of water and acetone (50 : 50 v/v) containing 1% PDMS for a period of 2 h. To prevent adverse effects due to the higher amount of silane on the mechanical properties of the formulated composites, 1% of silane was used.[18] Silane-treated empty-fruit-bunch fibers (STFs) were left in air for 24 h to complete the condensation reaction, after which they were dried in an oven for 8 h at 60°C and stored in plastic bags for further analysis. The dried fibers were cut into a length of 2–3 mm for the compounding process. The diameters of the untreated fibers were 0.14–0.15 mm, whereas the diameters of the treated fibers were found to be 0.11–0.12 mm.

The composites were fabricated from untreated or treated EFB fibers and PLA, with each composite category containing 30 wt % fiber. A primary screening of the extrusion process was carried out to understand the maximum loading of the fiber that could easily be extruded. We found that up to 30% fiber could be loaded into PLA with a smooth extrusion process. Greater fiber loadings were found to be difficult to extrude. The fibers (90 g) were mixed with PLA (210 g) and were fed into the extrusion process at 190°C. The extruded samples were cut to 2–3 mm in size and fed into injection-molding process at the same temperature. Samples prepared for further studies included raw empty-fruit-bunch fibers (RFs), UTFs, STFs, pure PLA, poly(lactic acid)/raw empty-fruit-bunch composites (PRFCs), poly(lactic acid)/ultrasound-treated empty-fruit-bunch

composites (PUTFCs), and poly(lactic acid)/silane-treated empty-fruit-bunch fiber/poly(lactic acid) composites (PSTFC).

Mechanical Testing. Tensile testing was conducted on the PLA/EFB composites before and after degradation tests. The preparation of the tensile test samples was carried out according to ASTM 638-08. The dimensions of the samples were 125 × 12.5 × 3.3 mm^3. Testing was carried out on tensile samples with a 65-mm gauge length with a Shimadzu universal tensile machine (model AG-1) with a 5-kN load cell running at a crosshead speed of 10 mm/min. The averages were taken for five replicate samples to obtain the tensile strength (TS) and tensile modulus (TM) for each category of composites.

Scanning Electron Microscopy (SEM). The surface morphology of the EFB fibers before and after modification and the surface morphology of the tensile samples of the PLA/EFB composites before and after exposure to natural degradation conditions were examined. The observation was carried out with the help of a Zeiss EVO 50 scanning electron microscope. The test samples were initially air-dried to make them moisture-free, after which they were sputter-coated with gold before SEM observation to prevent electrical discharges during testing.

Fourier Transform Infrared (FTIR) Spectroscopy. Functional group analysis was carried out for the EFB fibers before and after modification. This was also performed for a representative PLA/EFB composite before and after exposure to natural degradation conditions. An FTIR spectrophotometer (model THERMO) fitted with OMNIC software was used to obtain the IR spectrum with the standard KBr technique with a scanning wavelength range of 700–4000 cm^{-1}.

Density Measurement. Density measurement was conducted for the RFs, UTFs, and STFs and their respective composites to obtain the mass occupied by a unit volume of the sample. Density measurement was carried out with the help of a gas pycnometer (model Mycromeritics, AccuPyc 11 1340). Inert helium gas was allowed to pass through each sample, which weighed about 2–4 g. From the density data, the volume fraction of the void (V_v) within the composites was calculated with eq. (1):[2]

$$V_v = 1 - \rho_c \left(\frac{W_{\text{fiber}}}{\rho_{\text{fiber}}} + \frac{W_{\text{matrix}}}{\rho_{\text{matrix}}} \right) \quad (1)$$

where ρ_c is the composite density; W_{fiber}, W_{matrix}, ρ_{fiber}, and ρ_{matrix} are the weight percentages of the fiber (%), the weight percentage of the matrix (%), the density of the fiber (g/cm^3), and the density of the matrix (g/cm^3), respectively.

Water Uptake Analysis. Water uptake analysis was carried out on an injection-molded tensile sample of the PLA/EFB composite to study the moisture resistance capacity of the composites with respect to the fiber treatment. The tensile samples were immersed in distilled water at room temperature for a period of 150 days. The initial weight of the samples was noted before immersion, and the weights were taken for each sample at regular time intervals. The water uptake (%) was determined from eq. (2) as follows:

$$\text{Moisture content } (\%) = \frac{W_f - W_i}{W_i} \times 100 \quad (2)$$

where W_i is the initial weight taken for the sample before immersion and W_f is the final weight after immersion for a particular period.

Soil Burial Analysis. Outdoor soil burial analysis was carried out by the placement of the tensile samples of the PLA and PLA/EFB composites under soil for a period of 6 months. Test samples were buried at a depth of 10 cm with a regular supply of water to keep the soil moist. The samples were taken out at regular time intervals for SEM examination. After the burial period, the samples were washed with distilled water, lightly wiped with tissue paper, and dried to a constant weight at 60°C before measurements were taken for the final weight. The overall weight loss (W_{loss}) with respect to soil burial was determined as follows:

$$W_{\text{loss}} = \frac{W_{\text{initial}} - W_{\text{final}}}{W_{\text{initial}}} \times 100 \quad (3)$$

where W_{initial} is the weight of the sample before soil burial and W_{final} is the weight of the sample after soil burial. Tensile testing was conducted on samples after the burial period as described previously. Because water absorption is one of the major contributing factors toward the natural degradation of polymer composites, the diffusion coefficient for each composite category was also calculated with eq. (4) as follows:[19]

$$\text{Diffusion coefficient} = \pi \left(\frac{h}{4M_m} \right)^2 \left(\frac{M_{\text{final}} - M_{\text{initial}}}{\sqrt{t_{\text{final}}} - \sqrt{t_{\text{initial}}}} \right)^2 \quad (4)$$

where h is the thickness of the sample (mm), M_{initial} and M_{final} are the mass concentrations of moisture before and after analysis, respectively; M_m represents the level of saturation; and t_{initial} and t_{final} represent the initial and final times of analysis, respectively. By plotting the graph of the mass gain due to water sorption versus the square root of time, the diffusion coefficient can be evaluated as the slope of the line:[20]

$$\text{Diffusion coefficient} = \pi \left(\frac{h}{4M_m} \right)^2 (\text{Slope of regression line})^2 \quad (5)$$

RESULTS AND DISCUSSION

FTIR Analysis of the Fibers

The FTIR Spectra for the RFs, UTFs, and STFs are illustrated in Figure 1. Spectra for the fibers before and after surface modification were observed to be similar in many ways. Some of the conspicuous peaks included the broad peak at 3500–3200 cm^{-1}; this represented the characteristic stretching vibrations of bonded —OH groups (circled). The peak around 2925 cm^{-1} represented the stretching vibrations of the methyl and methylene components of the EFB fibers. The splitting observed for this peak with respect to the treated EFB fibers suggested a certain structural modification to the fiber; this was perhaps due to the removal of certain noncellulosic components from the fibers after treatment. Specifically, the spectrum for the STF fibers also revealed a certain peak at 864 cm^{-1}, which is often attributed to Si—O asymmetric stretching in Si—O—Si or cellulose —O—Si bonds.[21] The presence of this peak suggested that some condensation reactions might have occurred between the

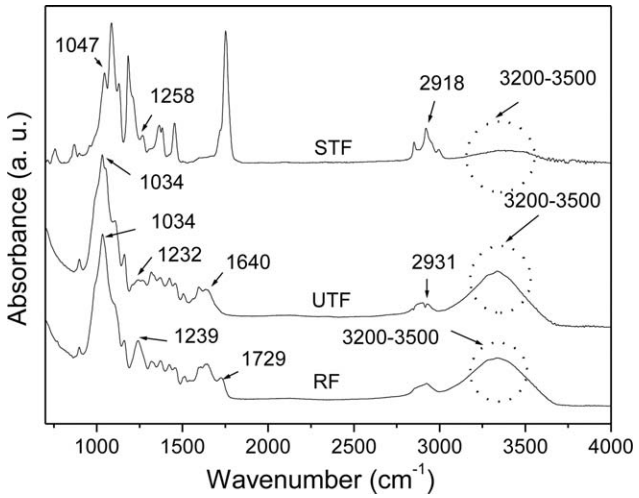

Figure 1. FTIR spectra of the RFs, UTFs, and STFs.

cellulose —OH groups of the fiber and hydrolyzed silane because of the treatment with PDMS. A similar peak was also observed for silanized jute fibers by other researchers.[22] Overall, the most conspicuous change to the spectra of the RFs with respect to fiber treatment was the disappearance of the peak around 1729 cm^{-1} from the spectra of the UTFs and STFs. This peak was attributed to the carbonyl (C═O) stretching of the acetyl and carboxylic acid components of the hemicellulose and lignin portions of the EFB fibers.[23] The disappearance of this peak could be attributed to the removal of a reasonable portion of hemicellulose and lignin from the EFB fibers with respect to surface modification. Furthermore, this suggests that surface modification might have enhanced the ionization of EFB —OH groups to alkoxide, as stated in the literature.[7] The presence of a large number of cellulose hydroxyl groups in natural fibers was the major contributing factor toward the fiber hydrophilic tendencies. Ionization of these hydroxyl groups therefore reduced the inherent hydrophilic properties of the fibers. This was a highly desirable phenomenon because the reduced hydrophilicity of the EFB fibers due to fiber treatment could enhance the compatibility between the fiber and hydrophobic polymer matrices. Moreover, there was a higher possibility for reduced biodegradation of composites when the reinforcing fibers were surface-modified.[24]

SEM Analysis of the Fiber

Figure 2 shows the SEM images of the RFs, UTFs, and STFs. The surface of the RF [Figure 2(i)] was composed of covered pores with a large portion of debris on the surface. Some of the materials covering the fiber surface might include noncellulosic substances, such as pectin, wax, and lignin. UTFs [Figure 2(ii)] can, however, be seen to reveal open pores with cleaner and rougher surface morphologies. This indicated that certain proportions of noncellulosic materials were removed through ultrasound treatment. The removal of these materials was necessary to enhance the EFB/PLA interfacial adhesion as it facilitated the bonding reaction and mechanical interlocking between the fiber and matrix due to exposure of the fiber cellulosic —OH to PLA matrix.[24] Furthermore, the removal of the noncellulosic components could lead to the structural modification of the fiber such that the chemical composition is restructured to become less susceptible to biodegradation. For the STFs in Figure 2(iii), the impartation of PDMS on the fiber surface manifested in the form of light films upon the opened pore spaces. This was significant because it helped to weaken the hydrophilic tendencies of the fiber through a reduction in the number of persistent hydroxyl groups on the fiber surface via a condensation reaction. The compatibility between the PLA matrix and EFB fibers, therefore, increased more.[25] In effect, the biodegradation of composites reinforced with these fibers could be greatly reduced, and they would also reveal a reduced weight loss, even after exposure to environmental conditions, as reported elsewhere.[24]

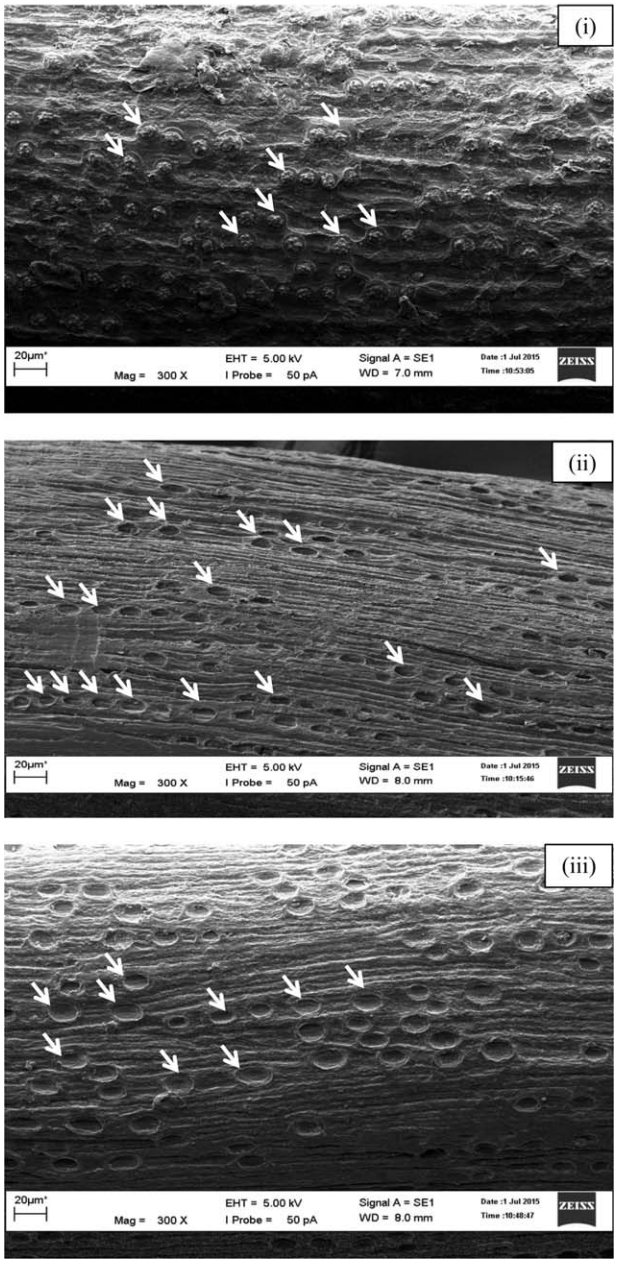

Figure 2. SEM images for the (i) RFs, (ii) UTFs, and (iii) STFs.

Table I. Densities Values Measured for the EFB Fiber and PLA/EFB Composites

Fiber code	Density (g/cm^3)	Composite code	Density (g/cm^3)
RF	1.3910	PLA	1.2576
UTF	1.4916	PRFC	1.3003
STF	1.4672	PUTFC	1.3207
		PSTFC	1.3438

Density of the Fibers and Composites

The density values measured for the RFs, UTFs, STFs, PLA, PRFCs, PUTFCs, and PSTFCs are presented in Table I. Among the fiber types, the UTFs possessed the highest density followed by the STFs, and the lowest density belonged to the RFs. The higher density of the UTFs compared to the RFs could perhaps have been due to the removal of noncellulosic portions, such as lignin, waxes, and hemicellulose from the fiber after treatment with ultrasound. This might have led to some structural modifications within the fiber and favored the crystalline cellulose, causing it to rearrange in a more ordered structural manner. The reordering could, therefore, increase the bulk density by reducing the surface volume.[26,27] As for the lesser density of the STFs compared to the UTFs, the reason for this could be associated with some direct condensation reaction; this might have occurred between the silane (PDMS) and cellulose —OH groups of the fiber, as reported elsewhere for silanized jute fibers.[22] Most often, silane treatment tends to reduce the number of available crystalline cellulose through a certain disruption of the cellulose arrangement. This could, therefore, favor more of the amorphous cellulose and invariably leads to the reduced overall fiber density.[26]

On the other hand, the density of PLA and the composites can be seen to follow the order PLA < PRFC < PUTFC < PSTFC. Obviously, all of the composite possessed higher densities than PLA; this could have been due to the higher density of the EFB fibers (1.3910, 1.4916, and 1.4672 g/cm^3 for the RFs, UTFs, and STFs, respectively) compared to PLA (1.2576 g/cm^3). This also conforms to the finding of other researchers, who reported higher densities of composites with increasing fiber content,[28] and therefore associated the increasing density with the higher density of the fiber at a higher loading. However, among the composite categories, the treated fiber composites possessed higher densities. This suggested the effective removal of less significant noncellulosic components from the fiber surface and might have increased the surface adhesion between the PLA and the fiber. This increased interfacial adhesion through reduced fiber size (diameter) could permit more of the fiber to occupy a lesser volume. Thus, the overall bulk density of the composites based on the treated fibers could, therefore, be higher than those of the composites based on untreated fibers.[26] We also found that the PSTFCs possessed higher densities than the PUTFCs. The reason for this could have been due to the greater possibility for the transcrystallinity of the STFs within the polymer matrices; this often made the density of the STF-based composites to be notably raised. The transcrystallinity of kenaf fibers within the polypropylene matrix was also reported elsewhere.[29]

FTIR Analysis of the Composites

Because all of the buried composites revealed similar spectra, an exemplary spectrum for the most degraded composite (PRFC) before and after soil burial is presented in Figure 3. The general observed peaks included a broad peak from 3500 to 3200 cm^{-1}, which represented H-bonded —OH stretching. This was shifted to a higher wavelength with a broader peak after the degradation test; this suggested an increase in the number of hydrogen bonds, perhaps because of interactions between —OH groups of the fiber and water molecules during the analysis period. During composite fabrication, surface interaction between the PLA and EFB fibers often arise as a result of hydrogen bonding between the EFB —OH groups and C=O from the ester linkage in PLA.[7] One could, therefore, suggest that the biodegradation of the PLA/EFB composites might have occurred through the cleavage of the hydrogen bonding. The cleavage of this bond invariably led to the presence of excess polar hydroxyl groups on the composite interface when it was being solvated by water in the soil. Thus, hydrogen bonding with water was favored. The peak around 2900 cm^{-1} was assigned to the C—H stretching vibrations of the methyl and methylene components of the EFB fiber cellulose and hemicellulose. This was observed to have shifted to a lower wavelength after biodegradation and suggested the possible degradation of a certain portion of the amorphous components of the EFB fibers during the soil burial period. The appearance of the peak around 1600 cm^{-1} after the soil burial period suggested that the hydrolysis of ester bonds in PLA might have produced some byproducts of degradation on the composite surface. The other observable change to the spectrum after biodegradation was the disappearance of the shoulder peak at 1128 cm^{-1}; this represented the C—O stretching of carboxylic acid and esters. This was attributed to the hydrolysis of the PLA ester bonds, which may have led to cleavage at the chain ends of PLA during soil burial. This might also have partly contributed to the degradation observed for the PLA/EFB composite as revealed by the SEM images.

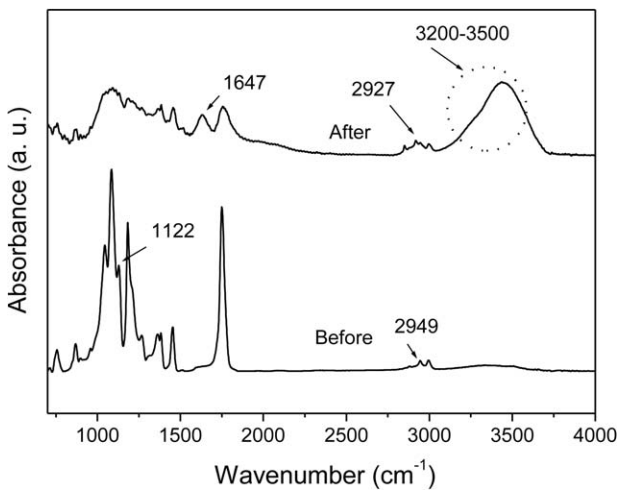

Figure 3. FTIR analysis of the PRFC before and after soil burial analysis.

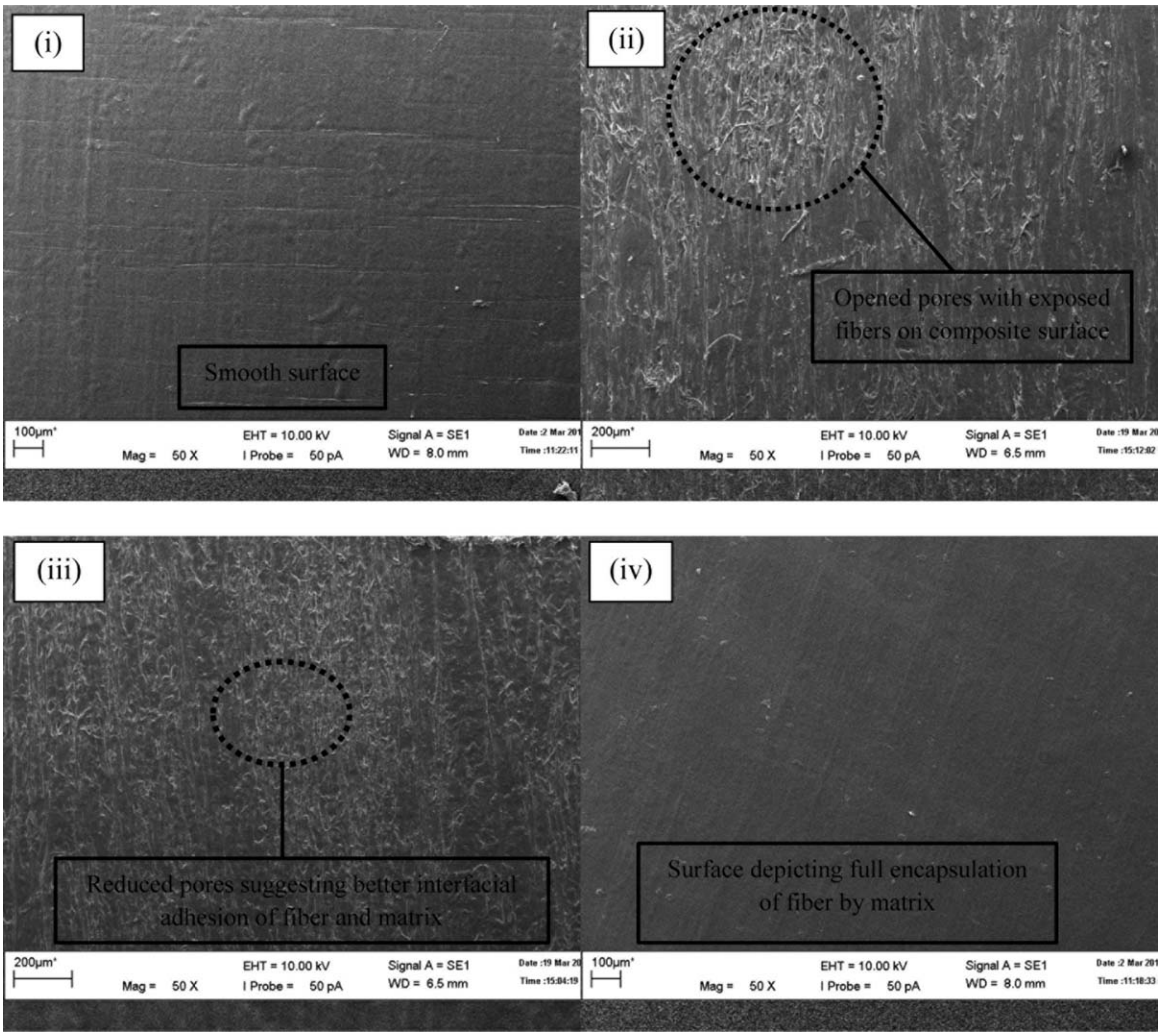

Figure 4. SEM images of the (i) PLA, (ii) PRFC, (iii) PUTFC, and (iv) PSTFC before soil burial.

SEM Analysis of the Composites

The SEM images of the outer surfaces of the PLA, PRFC, PUTFC, and PSTFC tensile samples before soil are shown in Figure 4. As expected, the surface of the PLA matrix was smooth to a large extent; this was perhaps due to the absence of reinforcing fillers in the sample. The surfaces of the PRFCs and PUTFCs were, however, composed of some opened pores. The greater number of pores and defects were found on the surface of the PRFCs; this indicated the improper encapsulation of the RFs by the PLA matrix. This suggested that there was poor wetting of the RF surface by the matrix during compounding; this was perhaps due to possible low interfacial adhesion between the surfaces of the hydrophilic fiber and its hydrophobic matrix counterpart.[24] The surfaces of the PUTFCs and PSTFCs were interestingly seen to reveal almost no opened pores; this suggested improved mechanical interlocking between the fiber and matrix. This might have been possible with the help of surface modification, which led to improved compatibility between the surfaces of the fiber and matrix, as reported elsewhere.[25]

On the other hand, the surface morphologies of the PLA, PRFCs, PUTFCs, and PSTFCs after partial degradation due to soil burial are revealed by the SEM images in Figure 5. As shown in these images, degradation began from the surface inward; this indicated that the depth of degradation experienced by each composite category depended on the susceptibility of its surface. The surface of the pure PLA [Figure 5(i)] was relatively smooth with not much significant degradation except for some slight surface erosion; this might have arisen from processing and handling during analysis. Most often, microorganisms that degrade PLA are not readily distributed in the natural environment, as explained in the literature.[30] This might, therefore, have reduced the susceptibility of PLA to microbial attack during the soil burial period. However, for all of the composites containing EFB fibers, various degrees of degradation were observed. This suggested that presence of EFB fibers and the interface of the EFB/PLA composite might have provided an avenue for water ingression into the composite and facilitated the growth of microbes; this, thereby, led to the gradual degradation of the matrix, as reported by other researchers.[31]

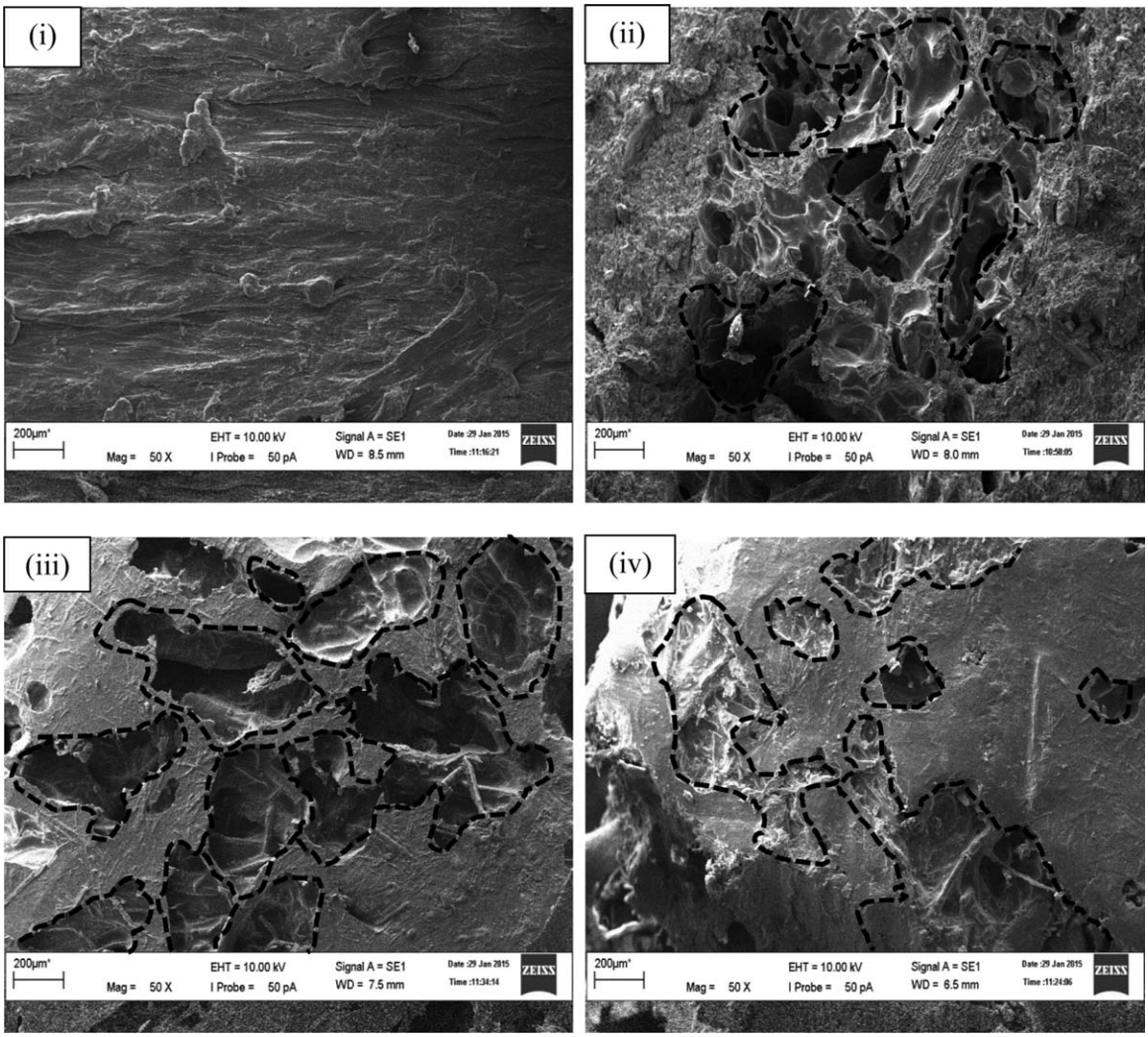

Figure 5. SEM images of the (i) PLA, (ii) PRFC, (iii) PUTFC, and (iv) PSTFC after soil burial.

Significant partial degradation was observed for the composites in the order PRFC > PUTFC > PSTFC. As a general observation, most of the microorganisms that are found in soils are mostly active toward hemicellulose, especially when environmental conditions are suitable for their growth.[32] This could have been the reason for the reduced biodegradation, as revealed by the treated-fiber-based composites; this was perhaps due to the initial removal of certain proportions of the hemicellulose during fiber treatment. Furthermore, the increased compatibility and interfacial bonding of the treated fiber with the PLA matrix might have served to strengthen the fiber–matrix interface and, thereby, prevented the ingress of water and restricted microbial growth on the composite surface. The slow degradation of PSTFC among other composites was, however, noteworthy and could be accrued to the condensation reaction; this reduced the number of pendant hydroxyl groups on the fiber surface as described previously. The fiber, therefore, became more hydrophobic as a result of the hydrophobic characteristics imparted by PDMS. With this, water molecules were effectively prevented from hanging on the composite surface such that there was no suitable environment for microbial growth on the composite surface.[32] In general, the nature of fiber modification and the nature of the surface were the major factors that influenced the biodegradation of the composites.

Weight Loss

The effect of soil burial on the overall weight loss of the PLA/EFB composites is summarized in Figure 6. Comparing the weight loss of these composites with that of the pure PLA matrix, we observed that there was reduced weight loss with respect to that of pure PLA (<1%) compared to the composites. The weight losses of the composites were in the order PRFC > PUTFC > PSTFC. The overall weight losses were 6.8, 5.0, and 3.7% for PRFC, PUTFC, and PSTFC, respectively. Because water sorption is one of the determinant factors for the degradation of the composites with respect to soil burial, the reduced weight loss of the treated-fiber-based composites, especially PSTFC, were attributed to the same effect discussed in the previous section. The diffusion of water into the composite could provide a suitable environment that could promote microbial activities and the hydrolysis of the composite material. The very low weight loss observed for PLA indicated

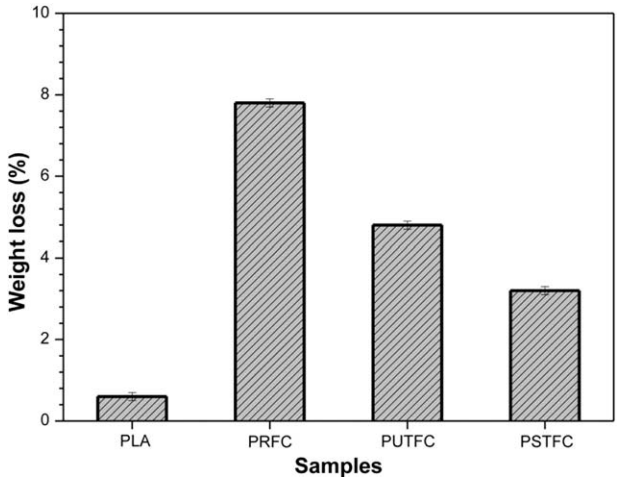

Figure 6. Effect of soil burial on the weight loss of the PLA and PLA/EFB composites.

reduced degradation of PLA, perhaps because of the slow hydrolysis rate of PLA, especially at reduced temperatures, as reported elsewhere.[33] On the other hand, the incorporation of EFB fibers increased the overall weight loss for the composites. This indicated that the presence of natural fibers raised the water sorption and created a rougher platform that could support the growth and activity of the microbes on the composite surface.[32] The possible mechanism of degradation of the composites could be depicted, as illustrated in Scheme 1.

Tensile Properties

Figure 7 shows the effect of soil burial on the tensile properties of PLA and its composites with treated and untreated EFBs. Both TS and TM followed the same pattern. There were observable decreases in TS and TM after the soil burial period. The largest drop in properties was obtained from the untreated fiber composite (PRFC), which showed up to about 27 and 35% reductions in TS and TM, respectively. This suggested that PRFC was more vulnerable to biodegradation compared to the treated fiber composites. This was attributed to the combined effect of the hydrolysis of the PLA matrix and the degradation of the PLA/EFB interface. As explained previously, the exposure of the EFB fibers on the surface of PRFC promoted the sorption

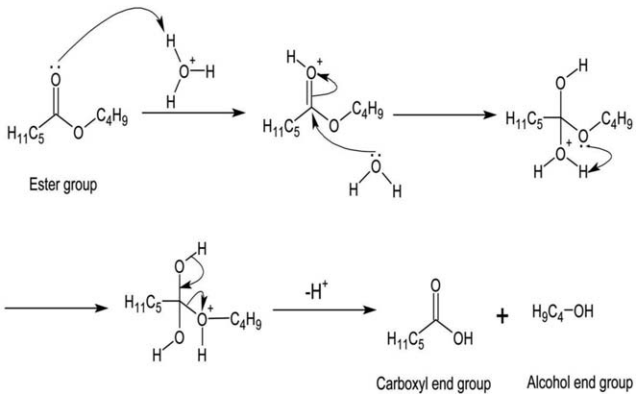

Scheme 1. Possible mechanism of degradation of the PLA-based composites.

of moisture by the composite. It also led to the formation of microcracks on the composite surface. The diffusion of water through these cracks via capillarity action adversely damaged the fiber–matrix interface and weakened the bond between the fiber and the matrix. In effect, the tensile properties of the composite were adversely affected.[34] In general, the observed decrease in the mechanical properties of the composites after degradation was associated with the possible presence of the void within the composite, especially for the untreated-fiber-based composites. The presence of these voids could have been a result of poor interfacial interlocking between the fiber and polymer matrix. These voids could, therefore, serve as concentration points for stress, such that there was a higher tendency for composite failure.

Void Content and Water Uptake Analysis

To establish the level of interfacial adhesion in the composites, the percentage void content was calculated with eq. (1). We found that the void contents of the composites were 4.22, 0.69, and 0.02% for PRFC, PUTFC, and PSTFC, respectively. Evidently, the number of voids in the composites was in the order PSTFC < PUTFC < PRFC. This explained the reason for the

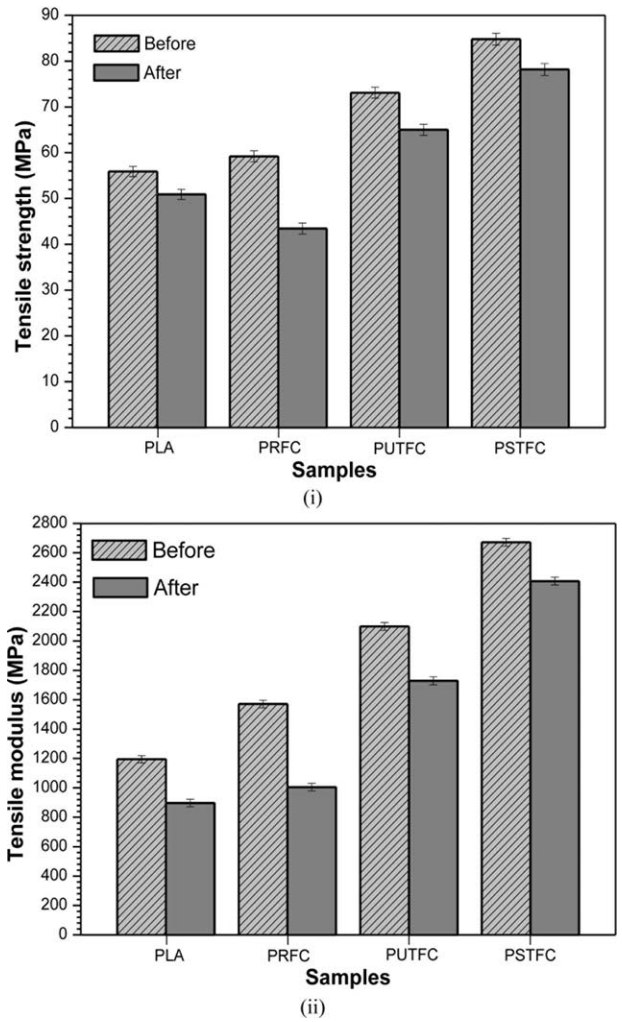

Figure 7. Effect of soil burial on the (i) TS and (ii) TM of the PLA and PLA/EFB composites.

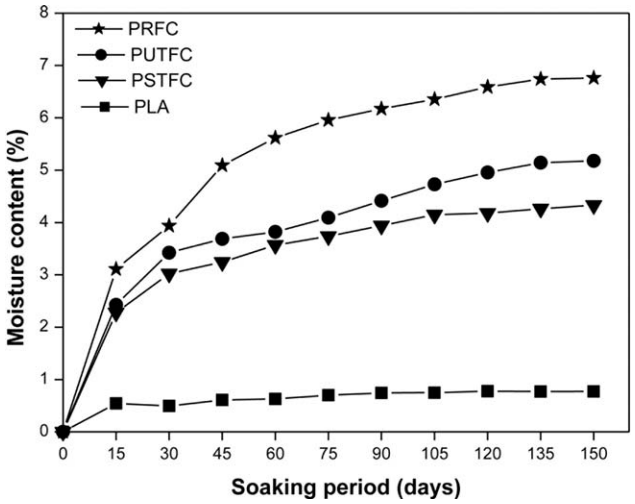

Figure 8. Variation of water absorption with soaking period for the PLA and PLE/EFB composites.

higher weight loss and larger percentage drop in the mechanical properties of the untreated-fiber-based composites (PRFCs). As water molecules diffused into these voids, the initial fiber–matrix adhesion became increasingly weakened; this led to the reduced mechanical properties in the composites. A similar observation was also reported by other researchers.[2,34,35] Furthermore, as reported in previous section, the rate of water diffusion into these cracks through the pore holes on the composite surface determined to a larger extent the rate of swelling within the composite. Swelling then caused the fibers to be forced out of the matrix, leaving behind holes, as revealed by the SEM images. These holes, therefore, hindered the effective transfer of stress along the composite length during mechanical testing and led to reductions in the tensile properties.

The water uptake values for the PLA and PLA/EFB composites are shown in Figure 8. Water sorption for all of the samples was observed to increase linearly as the soaking period increased with the initial rapid water uptake at the early stage of soaking. The water uptake depended on the hydrophilic nature of the fibers, the amount of fiber loading, the exposed area, the void content inside the composite, the surface protection, and interfacial adhesion between the fibers and the matrix.[36] There are three concepts established for the water uptake mechanism based on the relative mobility of the penetrant and the polymer segments because of their Fickian, anomalous, and intermediate behavior. According to Fickian behavior, the water uptake followed a faster rate followed by an equilibrium trend of absorption. The absorption decreased slowly as the soaking period increased further and tended toward saturation after a prolonged soaking period, conforming to a Fickian diffusion process. A similar phenomenon was also observed for kenaf-fiber-reinforced polypropylene composites during water absorption analysis by some other researchers.[29,37,38] All of the composites could also be seen to absorb more water compared to pure PLA, and the trend of water absorption for the composites was in the order PRFC > PUTFC > PSTFC. This phenomenon was attributed to the water uptake properties of the EFB fibers. Natural fibers manifest hydrophilic tendencies because of their abundant hydroxyl groups, which are able to interact with water molecules. The reduced water absorption was observed for the treated-fiber-based composites, with the largest reduction obtained from the STF composite (PSTFC). This was attributed to reduced hydrophilicity of the EFB fibers with respect to surface modification through ultrasound and silane treatment. The inherent hydrophilic nature of natural fibers often leads to swelling and increased water absorption of their thermoplastic composites when they are exposed to moisture. Worst still is the condition if there is poor adhesion between the fiber and polymer matrix.[39,40] Thus, the surface modification of the EFB fibers might have led to improved fiber–matrix interaction and effective bonding of the PLA matrix on the surface of the fiber, such that number of available pores through which water could diffuse into the composites was reduced. Interestingly, the silane-treated composites (PSTFC) revealed the lowest water absorption; this was perhaps due to the hydrophobic nature of PDMS combined with the coupling effect it rendered to the fiber–matrix interface. The coupling effect of PDMS might have enhanced the effective shielding of the EFB fibers by the PLA matrix such that few or no pores were opened for water diffusion into the composite. Also, the water-repelling tendency of PDMS might have prevented water molecules from hanging onto the composite surface and, thereby, reduced its absorption. This conformed to the suggestion elsewhere that a reduction in composite water absorption is highly achievable, mainly with compatibilizers, which tend to react with the —OH groups of the fiber.[41] On the other hand, the higher water absorption noticed for the untreated fiber composite (PRFC) could have been a result of the possible incomplete encapsulation of the RFs by PLA during compounding. This might have arisen from poor bonding at the interface of the untreated EFB fibers and the PLA matrix; this, thereby, led to exposure of the many fibers on the composite surface and a larger possibility for microvoids on the composite surface. The availability of more polar hydroxyl groups of the fibers on the surface of PRFC could, therefore, have been responsible for the formation of hydrogen bonds with water. Furthermore, the microvoids

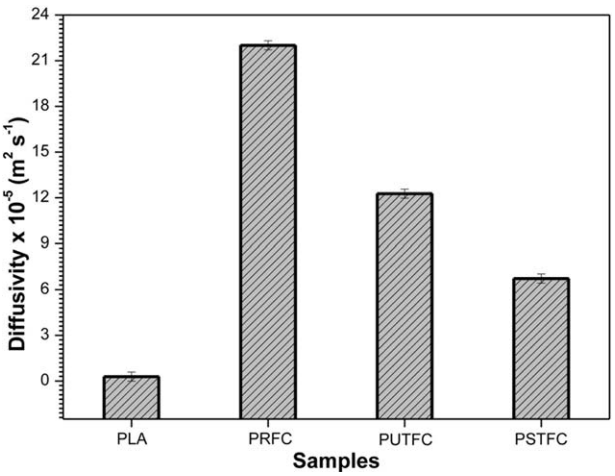

Figure 9. Diffusivity of water into the PLA and PLA/EFB composites during soil burial analysis.

served as diffusion points through which water molecules could flow into the composite and, thereby, increased the swelling and thickness of the composite.[42]

Furthermore, the diffusivity of water into the composites during soil burial period was calculated with eq. (4). Figure 9 represents the diffusion coefficient for each composite category on the basis of Fick's law of diffusion. The diffusivity of water into the samples followed the order PLA < PSTFC < PUTFC < PRFC. The reduced diffusivity of water into the STF-based composite (PSTFC) indicated the increased hydrophobicity of the composites with respect to fiber treatment with silane. The condensation reaction between the silane and hydroxyl groups of the fiber cellulose might have reduced the hydrophilic properties of the fibers and, thereby, reduced their tendency for water absorption. Overall, reduced water absorption would have helped restrict the swelling of the fibers within the composite, such that the mechanical properties could be retained, as confirmed by the tensile test results. This was because swelling often has adverse effects on the mechanical properties of natural fiber-reinforced composites. Composite swelling and fracture was reported elsewhere when kenaf fiber composites prepared with tributyl citrate plasticized cellulose acetate were immersed in water, and the resulting effect was reported to be reduced mechanical properties.[20] Similarly, from the mechanical properties results obtained herein, 27 and 35% reductions in TS and TM were observed for the PRFC compared to 8 and 11% (TS) and 9 and 17% (TM) reductions observed for PSTFC and PUTFC, respectively; this indicated a low level of swelling in the treated-fiber-based composites. This explained the improved retention of mechanical properties in the treated-fiber-based composites even after environmental exposure. Moreover, this might have been due the reduced disruption of the fiber–matrix interfacial adhesion of the composites due to less moisture absorption. The effects of other environmental factors and microbial activities on the treated fiber composites might also have been greatly reduced. This could perhaps have been due to the proper encapsulation of the fiber by the matrix because of the improved mechanical interlocking between the treated fibers and the polymer matrix.

CONCLUSIONS

EFB- and PLA-based composites were prepared through extrusion and injection-molding techniques. Before compounding, surface modification was performed through ultrasound and PDMS to improve the interfacial adhesion between the fibers and the matrix. The influence of surface treatment in terms of wettability and natural degradation stability was assessed by various testing methods. The surface treatment was found to cause structural changes in the fiber, as confirmed by SEM and FTIR analysis. The density of the fibers was found to be improved by the treatment. The reduced water absorption was observed for the treated-fiber-based composites because of the improved interfacial adhesion between the fibers and the matrix. The deterioration of the tensile properties was found to be maximum for the case of the RF-based composite, whereas PDMS treatment was found to decrease the initial water absorption of the PRFCs and thereby reduce the overall weight loss on one side. It also helped to retain the tensile properties of the composite on the other side. Thus, PDMS was active in preventing the undesirable biodegradation of the EFB/PLA composites.

ACKNOWLEDGMENTS

The authors show profound appreciation to the Ministry of Education, Malaysia, for financial support of this research with grant Fundamental Research Grant Scheme (FRGS) (RDU120106) and the Universiti Malaysia Pahang for financial contributions through Postgraduate Research Grant Scheme (PGRS) (GRS140343).

REFERENCES

1. Weng, Y. X.; Jin, Y. J.; Meng, Q. Y.; Wang, L.; Zhang, M.; Wang, Y. Z. *Polym. Test.* **2013**, *32*, 918.
2. Dhakal, H.; Zhang, Z.; Richardson, M. *Compos. Sci. Technol.* **2007**, *67*, 1674.
3. Li, X.; Tabil, L. G.; Panigrahi, S. *J. Polym. Environ.* **2007**, *15*, 25.
4. Ibrahim, N. A.; Abu-Ilaiwi, F.; Rahman, M. Z. A.; Ahmad, M. B.; Dahlan, K. Z. M.; Yunus, W. M. Z. W. *J. Polym. Res.* **2005**, *12*, 173.
5. Hill, C.; Abdul, H. *J. Appl. Polym. Sci.* **2000**, *77*, 1322.
6. John, M. J.; Anandjiwala, R. D. *Polym. Compos.* **2008**, *29*, 187.
7. Alam, A. K. M. M.; Beg, M. D. H.; Reddy Prasad, D.; Khan, M.; Mina, M. F. *Compos. A* **2012**, *43*, 1921.
8. Bouza, R.; Lasagabaster, A.; Abad, M. J.; Barral, L. *J. Appl. Polym. Sci.* **2008**, *109*, 1197.
9. Senawi, R.; Alauddin, S. M.; Saleh, R. M.; Shueb, M. I. *Int. J. Biochem. Biomater.* **2013**, *3*, 50.
10. Bax, B.; Mussig, J. *Compos. Sci. Technol.* **2008**, *68*, 1601.
11. Huda, M. S.; Drzal, L. T.; Mohanty, A. K.; Mishra, M. *Compos. Sci. Technol.* **2008**, *68*, 412.
12. Cadar, O.; Paul, M.; Roman, C.; Miclean, M.; Majdik, C. *Polym. Degrad. Stab.* **2012**, *97*, 354.
13. Leejarkpai, T.; Suwanmanee, U.; Rudeekit, Y.; Mungcharoen, T. *Waste Manage.* **2011**, *31*, 1153.
14. Kale, G.; Aurus, R.; Sing, S. P. *J. Polym. Environ.* **2006**, *14*, 317.
15. Kale, G.; Aurus, R.; Sing, S. P.; Narayan, R. *Polym. Test.* **2007**, *26*, 1049.
16. Ndazi, B. S.; Karlsson, S. *eXpress Polym. Lett.* **2011**, *5*, 119.
17. Espert, A.; Vilaplana, F.; Karlsson, S. *Compos. A* **2002**, *35*, 1267.
18. Goriparthi, B. K.; Suman, K.; Mohan Rao, N. *Compos. A* **2012**, *43*, 1800.
19. Christian, S.; Billington, S. *Compos B* **2012**, *43*, 2303.
20. Pang, C.; Shanks, R. A.; Daver, F. *Compos. A* **2015**, *70*, 52.
21. Khan, M. A.; Hassan, M. M.; Taslima, R.; Mustafa, A. *J. Appl. Polym. Sci.* **2006**, *100*, 4361.
22. Hong, C.; Hwang, I.; Kim, N.; Park, D.; Hwang, B.; Nah, C. *J. Ind. Eng. Chem.* **2008**, *14*, 71.

23. Chowdhury, M. N. K.; Beg, M. D. H.; Khan, M. R.; Mina, M. F. *Cellulose* **2013**, *20*, 1477.
24. Liu, L.; Yu, J.; Cheng, L.; Yang, X. *Polym. Degrad. Stab.* **2009**, *94*, 90.
25. Soykeabkaew, N.; Supaphol, P.; Rujiravanit, R. *Carbohydr. Polym.* **2004**, *58*, 53.
26. Lee, C.-K.; Cho, M. S.; Kim, I. H.; Lee, Y.; Do Nam, J. *Macromol. Res.* **2010**, *18*, 566.
27. Karina, M.; Onggo, H.; Abdullah, A. D.; Syampurwadi, A. *J. Biol. Sci.* **2008**, *8*, 101.
28. Katsoulotos, G.; Pappa, G.; Tarantili, P.; Magoulas, K. *Polym. Eng. Sci.* **2008**, *48*, 902.
29. Islam, M. R.; Beg, M. D. H.; Gupta, A.; Mina, M. F. *J. Appl. Polym. Sci.* **2013**, *128*, 2847.
30. Rudnik, E.; Briassoulis, D. *Ind. Crops Prod.* **2011**, *33*, 648.
31. Petinakis, E.; Liu, X.; Yu, L.; Way, C.; Sangwan, P.; Dean, K.; Bateman, S.; Edward, G. *Polym. Degrad. Stab.* **2010**, *95*, 1704.
32. Alvarez, V.; Ruseckaite, R.; Vazquez, A. *Polym. Degrad. Stab.* **2006**, *91*, 3156.
33. Shogren, R.; Doane, W.; Garlotta, D.; Lawton, J.; Willett, J. *Polym. Degrad. Stab.* **2003**, *79*, 405.
34. Upadhyaya, P.; Garg, M.; Kumar, V.; Nema, A. K. *Mater. Sci. Appl.* **2012**, *3*, 317.
35. Costa, F. H. M. M.; D'Almeida, J. R. M. *Polym.–Plast. Technol. Eng.* **1999**, *38*, 1081.
36. Mina, M. F.; Sharmin, S.; Rummana, M. *Polym. Degrad. Stab.* **2009**, *94*, 183.
37. Ellyin, F.; Maser, R. *Compos. Sci. Technol.* **2004**, *64*, 1863.
38. Islam, M. R.; Rivai, M.; Gupta, A.; Beg, M. D. H. *J. Polym. Eng.* **2014**, *35*, 135.
39. Nanda, M. R.; Misra, M.; Mohanty, A. K. *Macromol. Mater. Eng.* **2012**, *297*, 184.
40. Abdelmouleh, M.; Boufi, S.; Belgacem, M. N.; Dufresne, A. *Compos. Sci. Technol.* **2007**, *67*, 1627.
41. Lee, B. H.; Kim, H. S.; Lee, S.; Kim, H. J.; Dorgan, J. R. *Compos. Sci. Technol.* **2009**, *69*, 2573.
42. Shinoj, S.; Visvanathan, R.; Panigrahi, S.; Kochubabu, M. *Ind. Crops Prod.* **2011**, *33*, 7.